# Kinematical x-ray diffraction model with a new boundary condition for analysis of Bragg-peak profiles of layered crystals

C. R. Wie and H. M. Kim
*State University of New York at Buffalo, Department of Electrical and Computer Engineering and Center for Electronic and Electrooptic Materials, Bonner Hall, Buffalo, New York 14260*

(Received 2 October 1990; accepted for publication 22 January 1991)

A new boundary condition is employed in the kinematical model analysis of Bragg-peak profiles of layered single crystals, which is the dynamical reflection amplitude of the substrate instead of the previously used dynamical intensity. It is shown that this boundary condition properly accounts for the angular shift effect in the Bragg-peak profile of very thin epitaxial layers and superlattices. A kinematical model simulates properly the interference profiles in the *C*-layer Bragg peak of *C/A/C/sub*-type samples, but not in the *B*-layer Bragg peak of the *B/A/B*-type samples. The simulated and experimental rocking curves for the thin single-layer AlGaAs/GaAs and GaInAs/InP samples and for an AlGaAs/GaAs superlattice sample are discussed. Rocking curves are simulated by using the dynamical diffraction theory and the kinematical model with the old or new boundary condition. A matrix method for the dynamical theory superlattice simulation is also presented. The superlattice simulation using this matrix method is found to be substantially faster than the conventional recursive formula approach.

## I. INTRODUCTION

Double crystal x-ray diffractometry along with Rutherford backscattering spectrometry (RBS) is a suitable nondestructive technique for characterizing the strain and composition depth profiles in single-crystal samples having depth nonuniformities. The x-ray rocking curve technique has been used widely for analyzing semiconductor heteroepitaxial structures,[1-5] superlattices (SL),[6-9] thermally diffused samples,[10,11] keV or MeV ion-implanted samples,[12-14] and implanted magnetic garnet materials.[15,16] Recently, this technique has been used successfully in characterizing buried ultrathin strained layers such as the GaInP layer in InP/GaInP/InP samples[17] and the Ge layer in Si/Ge/Si samples[18] by making use of the x-ray interference structure in the rocking curves. The RBS channeling technique was also used for characterizing very thin semiconductor layers.[19] The RBS technique using the MeV He ions, however, can introduce a beam-induced lattice strain during the alignment and measurement process,[20] and therefore care must be taken to avoid such effects in the final result. The nanometer epilayer thickness can also be measured by grazing-incidence x-ray diffraction.[21,22]

In the past 15 years or so, many papers have appeared concerning the theoretical analysis of the rocking curve data. The analysis objective was to derive the strain, composition, and/or damage depth profiles from the experimental data. In general, the process involves using an assumed strain depth profile in the x-ray-diffraction model and calculating a theoretical curve. The best fit to the experimental rocking curve is taken as the actual profile. The methods of calculating theoretical rocking curves included the dynamical theory, solving the Takagi–Taupin equation[23] by numerical integration[4,12] or by using the recursive formula employing an analytic solution,[7,14,24] and a simplified computation scheme partly using the kinematical model.[25] This kinematical model was successfully used in analyzing the rocking curves from keV ion-implanted semiconductors[13] and ferrimagnetic garnet materials,[25] and superlattices.[6,28] Often, the kinematical model provides a more clear physical insight and a faster rocking curve simulation.

However, it was recently observed for thin heteroepitaxial samples[3] and thin SLs[26] that the previously used kinematical model resulted in a discrepancy from the corresponding dynamical theory calculation. The discrepancy occurs in the Bragg-peak position of a thin epilayer and in the zeroth-order SL peak position. This is an important observation because the lattice strain and chemical composition profiles are determined from the angular distance of the layer Bragg-peak profile from the substrate Bragg-peak position. We reported that the angular shift is caused mainly by the interference effect between the reflection amplitude by the layer (or superlattice) and the amplitude by the substrate.[27]

The kinematical calculations in the previously published papers were based on a model[25] that combines the layer diffraction amplitudes, which are in a kinematical approximation, with the dynamical diffraction intensity of the substrate, using appropriate absorption and phase factors for each layer. This type of kinematical model cannot properly account for the interference effect between the layer and substrate. The kinematical approximation is valid only if the total thickness of the layers is substantially less than the primary extinction length of x rays in the material, whereas the interference effect produces a peak shift for such small thicknesses.[3,26,27] Therefore, if a kinematical model is to be used for the rocking curve simulation, a proper layer-substrate phase relationship should be taken into account.

The objective of this paper is to introduce a kinematical diffraction model with a correct layer-substrate phase relationship. A natural approach is to use the substrate (dynamical) amplitude instead of the dynamical intensity as the boundary condition and to find an appropriate kinematical

 0021-8979/91/096406-07$03.00  

expression for the layer. Rocking curves calculated using this kinematical model with the amplitude boundary condition (ABC) are compared with those calculated using the kinematical model with the intensity boundary condition (IBC) as well as those obtained by using the dynamical theory. The rocking curve profiles are discussed, using the calculated curves and some experimental data for thin single-layer samples, AlGaAs/GaAs and GaInAs/InP, and for a thin SL sample of AlGaAs/GaAs. We also discuss the sample structures that manifest interference profiles in the Bragg peak. We show that our ABC kinematical model shows the same Bragg peak profile and the zeroth-order SL peak profile as the dynamical theory does, properly showing the peak shift effect. Also, the ABC kinematical model is shown to agree with the dynamical theory in the relative profile of the x-ray interference structure that appears in the $C$-layer Bragg peak of the $C/A/C/B$(substrate)-type structures. However, our ABC kinematical model is shown to deviate substantially from the corresponding dynamical calculation of the interference profile in the $B$-layer Bragg peak of the $B/A/B$(substrate)-type structures.

## II. CALCULATION OF ROCKING CURVES

### A. Rocking curve calculation using dynamical theory

In this section, we briefly review the dynamical diffraction theory that is used here for rocking curve calculation. Diffraction of an incident plane-wave x-ray beam by a layered single crystal can be described by an analytic solution or a numerical integration of the Takagi–Taupin equation.[23] An analytic solution to the Takagi–Taupin equation is given in the Appendix for the normal polarization in the Bragg case. The method of rocking curve simulation consists of introducing a model strain in the Takagi–Taupin equation, governing x-ray propagation in distorted crystals, in order to obtain a simulated reflection profile. The choice of computation scheme largely depends upon the strain description. For ideally sharp junctions where the strain is a steplike function, it is more appropriate to use the analytic solutions (given in the Appendix) than the numerical integration procedure. This type of strain profile is relevant for sharp-junction heteroepitaxial layers and superlattices.

The boundary condition taken by most authors is that the reflection amplitude is zero at the under surface of the substrate. With this boundary condition, the Takagi–Taupin equation is numerically integrated over the substrate to yield the amplitude at the top surface of the substrate. However, an analytical expression of the dynamical amplitude at the substrate top surface was obtained:[14]

$$X_0 = -B/(C-S), \tag{1}$$

where $|X_0|^2$ is the reflectivity of a bulk substrate and $B$, $C$, and $S$ are structural parameters defined in the Appendix. This expression gives the same reflection profile as the numerical integration procedure does.

For an isolated single-crystal plate, the diffraction amplitude may be obtained from Eq. (A2) by letting $X(z_{j-1}) = 0$ and $z_j - z_{j-1} = -t$ where $t$ is the thickness,

$$X = \frac{-iB\tan(SAt)}{S + iC\tan(SAt)}. \tag{2}$$

We use this equation to derive kinematical approximation.

The formulas (1) and (2) and those given in the Appendix are for the normal polarization only. The formulas (1) and (A2) can constitute the dynamical theory in the Bragg case for a layered single crystal (or in the layer approximation). In the double crystal geometry, the beam incident to the second (sample) crystal is usually dominated by the normal polarization and therefore, for the sake of simplicity, we considered only the normal polarization in the formulas. In order to fit the experimental rocking curves, the plane-wave rocking curve, $|X|^2$ vs $\theta$, was convolved with an appropriate Gaussian convolution function to fit the experimental broadening.

For samples in which the strain profile varies gradually as in a graded buffer layer, in samples with interface transition regions, in ion-implanted samples, and in thermally diffused samples, a direct numerical integration of the Takagi–Taupin equation could be more appropriate. This approach was taken by Larson and Barhorst[12] for implanted and annealed Si single crystals, and by Fukuhara and Takano[10] for thermally diffused Si crystals. However, the procedure followed by most authors, even for samples with gradually varying strains, consisted of dividing a region with the varying strain into slabs of constant strain (layer approximation) and applying the analytic solution recursively to each slab. This approach was taken, for example, for the implantation strain,[14] and semiconductor heterojunctions with a graded buffer layer.[24]

### B. Kinematical diffraction model

We present in this section a semikinematical model of x-ray diffraction by treating the epitaxial layers in a kinematical approximation and the substrate by the dynamical theory [i.e., Eq. (1)]. If a layer is thin enough so that $At \ll 1$, the diffraction amplitude Eq. (2) may be approximated as

$$X \cong i\exp(-iYAt)\sin(YAt)/Y. \tag{3}$$

This equation is the kinematical amplitude of a thin crystal plate, and has the same form as the optical Fraunhoffer diffraction by a single slit of width $t$. The amplitude given by $N$ layers is the sum of the amplitudes given by each layer, each being multiplied by adequate phase and absorption factors,

$$X_N = i\sum_{j=1}^{N} a_j \exp[-i(A_j Y_j t_j + \Phi_j)]\sin(A_j Y_j t_j)/Y_j, \tag{4}$$

where $a_j = \exp[-(\gamma_0 + |\gamma_H|)/2|\gamma_0\gamma_H|\Sigma_{i=j+1}^{N}\mu_i t_i]$ is the absorption factor, $\mu_i = \lambda r_e(f_0'' + f_H'')/V$ is the absorption coefficient for the $i$th layer, and $\Phi_j = 2\Sigma_{i=j+1}^{N} A_i Y_i t_i$ is the phase delay due to the layers above the $j$th layer. Eq. (4) is the same as the kinematical formula in Ref. 25 except that the phase delay $\Phi_j$ is modified so that the formula (4) can be directly combined with the dynamical substrate amplitude [Eq. (1)]. Including the substrate, a complete kinematical formula for a heteroepitaxial sample is

$$X_T = X_N + a_0\exp(-i\Phi_0)X_0, \tag{5}$$

where $X_0$ is the dynamical amplitude of the substrate given by Eq. (1). We name Eq. (5) the amplitude boundary condition (ABC) formula.[32]

In Sec. III, we show that Eq. (5) agrees with the dynamical theory in fitting the experimental data for very thin heteroepitaxial samples and in fitting the zeroth-order peak of a SL sample for which the peak shift effect is apparent. We also discuss an application of the ABC formula to the analysis of the interference profile in the Bragg peak for some particular sample structures.

### C. Matrix approach to the dynamical theory SL calculation

We present here a matrix method of rocking curve calculation for SLs in the dynamical theory. SL calculation using this method is substantially faster than the recursive formula approach especially for a large period superlattice and for investigating the interfacial strain effects. Our approach differs from Abeles's matrix method[33,34] which employs the Maxwell's equations formulated in a $2\times2$ matrix form whereas our approach starts with the analytical solution of the Takagi–Taupin equation.

The dynamical recursive formula in the Bragg case may be written as

$$X(z_j) = [P_j X(z_{j-1}) + Q_j]/[V_j X(z_{j-1}) + W_j], \qquad (6)$$

where the layer parameters $P$, $Q$, $V$, and $W$ are complex numbers and can be expressed by comparing Eqs. (6) and (A2) in terms of $A$, $B$, $C$, and $S$ which are given in the Appendix, and $X(z_j)$ is the reflection amplitude at the $j$th layer top surface. For a SL structure on a substrate or on any other structure, the dynamical amplitude on the SL top surface is

$$X_{SL} = (P_{SL} X_{under} + Q_{SL})/(V_{SL} X_{under} + W_{SL}), \qquad (7)$$

where $X_{under}$ is the dynamical amplitude at the SL under surface, for example, at the substrate top surface if no buffer layer is present. It can be shown for an $N$-period superlattice that

$$\begin{pmatrix} P_{SL} & Q_{SL} \\ V_{SL} & W_{SL} \end{pmatrix} = \begin{pmatrix} P_{period} & Q_{period} \\ V_{period} & W_{period} \end{pmatrix}^N, \qquad (8)$$

where

$$\begin{pmatrix} P_{period} & Q_{period} \\ V_{period} & W_{period} \end{pmatrix} = \begin{pmatrix} P_m & Q_m \\ V_m & W_m \end{pmatrix} \cdots \begin{pmatrix} P_2 & Q_2 \\ V_2 & W_2 \end{pmatrix} \begin{pmatrix} P_1 & Q_1 \\ V_1 & W_1 \end{pmatrix}, \qquad (9)$$

for an arbitrary $m$-layer period. These $2\times2$ complex matrices can be handled as $4\times4$ real matrices. From Eq. (8), it can be seen that the time consumed in the numerical calculation is practically constant, independent of the number of SL periods $N$. This is because the operation of the $N$th power may be performed after diagonalization of the period matrix. Using Eqs. (7)–(9), the dynamical theory SL rocking curves were calculated and are presented in the next section. For a large period superlattice or for considering interfacial layers (thereby increasing the number of layers in a period), this matrix approach can considerably reduce the computation time. For example in our calculation, using an IBM PC/XT compatible personal computer with a math coprocessor and Quick Basic, it took a constant time of 5 min, which becomes less than the time taken by the recursive formula approach at or above 8 periods for a four-layer period SL. For a two-layer period SL, the matrix approach took 1 min and 20 s, which is faster at or above 20 periods than the recursive formula approach.

## III. RESULTS AND DISCUSSION

### A. Single epilayer samples

Figure 1 shows the detailed analysis of the peak shift effect in the experimental rocking curves of a very thin layer sample. In Figs. 1(a) and 1(e), experimental data are shown that were taken from a successively etched 0.88-$\mu$m-thick $Al_{0.37}Ga_{0.63}As$/GaAs sample and a 0.65-$\mu$m-thick $In_{0.535}Ga_{0.465}As$/InP sample. The 004 rocking curves were taken in a double crystal geometry with Fe$K\alpha_1$ radiation that was reflected off the (004) planes of a GaAs(001) first crystal. The normal absorption coefficient of Fe$K\alpha_1$ is about $0.07\,\mu m^{-1}$ in GaAs. The simulated rocking curves using the ABC kinematical formula, Eq. (5), are also shown in Figs. 1(b) and 1(f); the dynamical formula, Eq. (A2), in Figs. 1(c) and 1(g); and the IBC kinematical formula in Figs. 1(d) and 1(h). It can be seen that both the dynamical formula and the ABC kinematical formula can fit the experimental data equally well, properly showing the peak shift effect as the layers become thinner. However, the IBC kine-

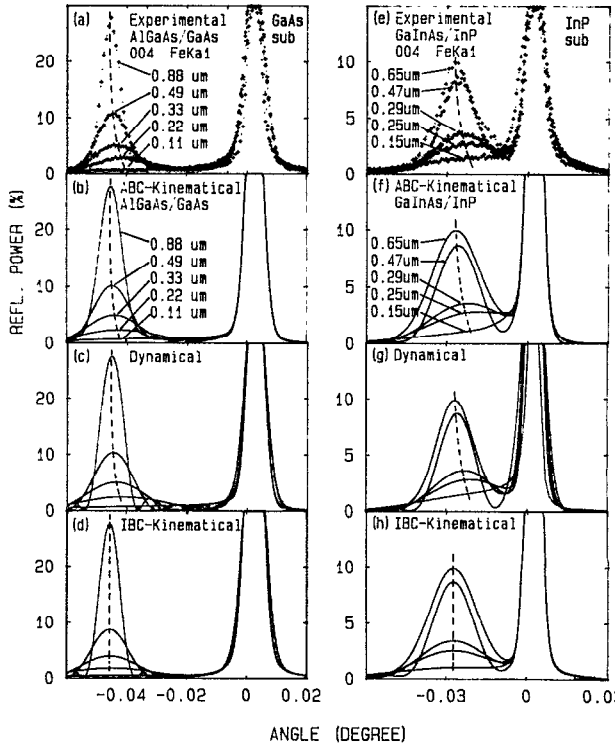


FIG. 1. (a)–(d) Experimental and simulated 004 rocking curves to illustrate the peak shift effect in the $Al_{0.37}Ga_{0.63}As$ layer peak on a GaAs(001) substrate; and (e)–(h) in the $Ga_{0.535}In_{0.465}As$ layer peak on an InP(001) substrate. Simulations by the dynamical theory or the ABC kinematical model show the peak shift effect, but the IBC kinematical model does not show the peak shift.

matical formula does not show the peak shift effect even at the smallest thickness calculated here. Figure 1 therefore shows that the ABC kinematical formula, but not the IBC formula, can be used for analysis of the detailed diffraction profiles of very thin layers.

In Fig. 2, we show the deviation in the epilayer peak intensity calculated by the ABC formula from that calculated by the dynamical formula. The rocking curves are 004 reflections of Fe$K\alpha_1$ radiation from a 0.7-, 0.9-, or 1.5-$\mu$m-thick $Al_{0.25}Ga_{0.75}As$/GaAs sample. For a layer thicker than 0.7 $\mu$m, the ABC formula gives an increasingly higher peak intensity than the dynamical formula does. This is expected from the facts that the kinematical approximation becomes less valid for thicker layers and that the kinematical formula tends to give a higher intensity than the dynamical counterpart does (see, for example, Fig. 2). Therefore, Figs. 1 and 2 show that the ABC kinematical model can be used for the detailed profile analysis if the epilayer is thin enough for a kinematical approximation to be valid.

### B. X-ray interference in *B/A/B*-type and in *C/A/C/sub*-type structures

We now discuss the applicability of the ABC formula to the analysis of interference profiles. Figure 3 shows the simulated 004 rocking curves around the GaAs substrate Bragg peak of a 0.5-$\mu$m GaAs/$t$-Å $Ga_{0.75}In_{0.25}As$/GaAs(001) buried pseudomorphic sample (*B/A/B* type). The GaAs cladding layer is 0.5 $\mu$m thick and the strained GaInAs is 24, 22, 20, or 18 Å thick. In this type of buried strained layer structure, the x-ray rocking curve shows an interference structure within the substrate Bragg peak profile. This occurs due to the phase difference between the wave reflected by the cladding GaAs layer and that by the substrate GaAs.[29,30] The phase difference is proportional to the thickness times mismatch product of the buried pseudomorphic GaInAs layer.[17] This interference structure was shown to be

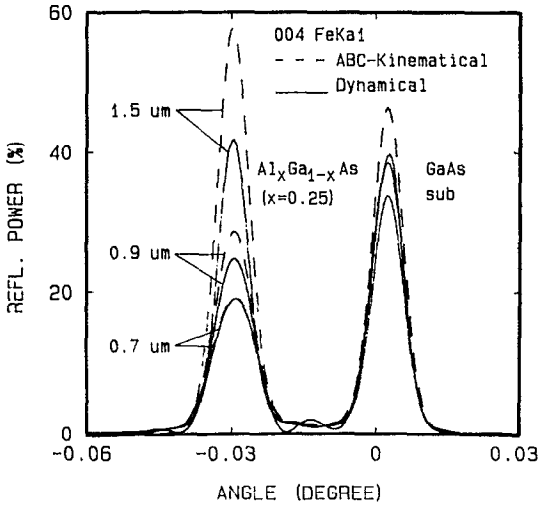


FIG. 2. The layer peak intensity of a single $Al_{0.25}Ga_{0.75}As$ epilayer on a GaAs(001) substrate becomes increasingly different in the ABC kinematical (dashed) and in the dynamical (solid) simulations with increasing layer thickness.

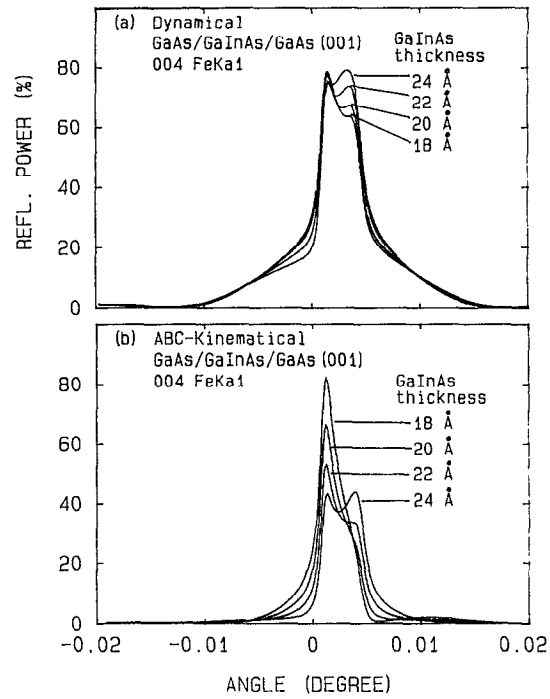


FIG. 3. The simulated GaAs 004 Bragg-peak profiles are shown for a differing $Ga_{0.75}In_{0.25}As$ layer thickness in a *B/A/B*-type 0.4-$\mu$m GaAs/GaInAs/GaAs(001) sample. The interference profile is significantly different between the dynamical and ABC kinematical simulations.

an effective tool in the heterostructure analysis with a submonolayer resolution, shown experimentally by Wie *et al.*[17], and independently by Tapfer *et al.*[18] It was theoretically predicted and explained by Wie,[29] Tapfer and Ploog,[35] and Holloway.[30] It can be seen in Fig. 3 that both the dynamical theory and the ABC kinematical formula exhibit an interference structure but they differ substantially from each other. A similar discrepancy was observed even when the cladding GaAs thickness was as small as 0.1 $\mu$m. This is because of the fact that the layer can be described by a kinematical approximation whereas the substrate requires an exact dynamical expression. Therefore, only the full dynamical theory can be used in analyzing the interference profiles of the *B/A/B*-type samples.

However, we show in Fig. 4 that the ABC formula can be used for the analysis of the interference profile in the C-layer Bragg peak of the *C/A/C/sub*-type samples for which the composition of the *C* layers is different from that of the substrate. Figure 4 shows the simulated rocking curves of a 0.4-$\mu$m $Al_{0.3}Ga_{0.7}As$/$t$-Å $Ga_{0.75}In_{0.25}As$/0.5-$\mu$m $Al_{0.3}Ga_{0.7}As$/GaAs(100) sample. It can be seen that the relative profile of the AlGaAs peak is very similar in the dynamical curve [Fig. 4(a)] and in the ABC kinematical curve [Fig. 4(b)]. The intensities of the AlGaAs layer peak profiles differ slightly from each other in the above two simulations. However, the absolute intensity of the simulated rocking curve peaks should be taken only in a relative and approximate sense because the simulated intensity does not accurately involve such factors as the actual amounts of normal and parallel polarizations in the incident beam, Debye–Waller factor of the sample, mozaic nature of the sample,

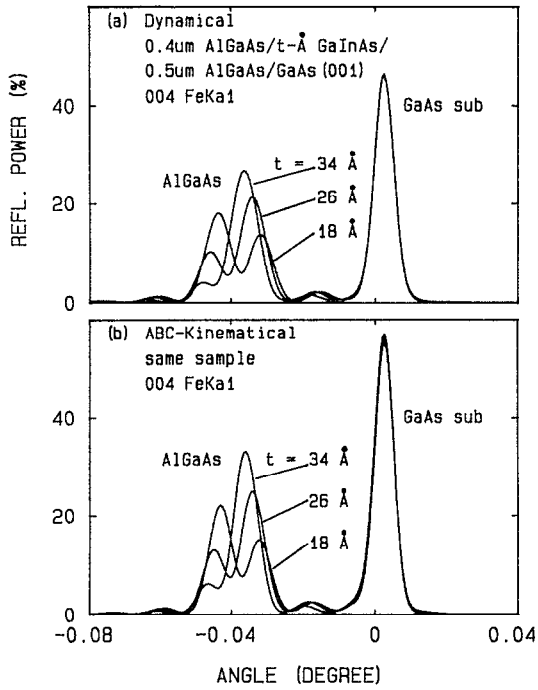


FIG. 4. The simulated AlGaAs 004 Bragg peak profiles are compared between the dynamical and ABC kinematical simulations. The sample is a *C/A/C/sub*-type 0.4-$\mu$m $Al_{0.3}Ga_{0.7}As/Ga_{0.75}In_{0.25}As$/0.5-$\mu$m $Al_{0.3}Ga_{0.7}As$/GaAs(001). It can be seen that the interference profiles from the two simulations are relatively the same.

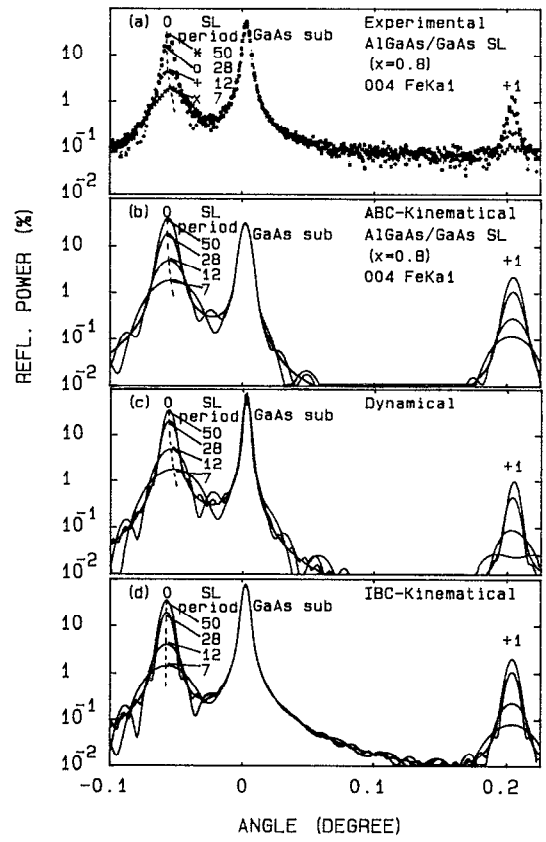


FIG. 5. Experimental and simulated 004 rocking curves are shown for a 146-Å $Al_{0.8}Ga_{0.2}As$/146-Å GaAs superlattice on a GaAs(001) substrate with a differing number of SL periods in the sample. The zeroth-order SL peak shifts toward the substrate GaAs peak for a smaller SL thickness. This effect will be more obvious for a SL with a lower Al content (or equivalently a lower mismatch). The IBC kinematical model does not show the peak shift effect. The dashed line in the zeroth-order SL peak indicates the peak position.

crystal defects, etc., which will affect the peak intensity. Therefore, we conclude that the ABC formula is valid for the x-ray interference analysis of the *A* layer in the *C/A/C/sub*-type samples, but not in the *B/A/B*-type samples. Also, since the layer expressions and their relative phases are essentially the same between the IBC and ABC kinematical formulas (the difference exists in the expression for the substrate), the IBC formula is equally valid for the analysis of *C/A/C/sub*-type structures.

### C. The zeroth-order SL peak

We now turn to the SL analysis. We will show that the ABC kinematical model properly simulates the peak shift effect in the zeroth-order SL peak, consistent with the dynamical calculation and the experimental data. Figures 5(b)–5(d) show the simulated 004 diffraction peaks of a 146-Å $Al_{0.8}Ga_{0.2}As$/146-Å GaAs SL sample with 50, 28, 12, or 7 SL periods. Calculations using the ABC kinematical model or the dynamical theory show the peak shift effect in the zeroth-order SL peak and agree with the experimental data that are presented in Fig. 5(a). For a SL sample with a smaller Al content (or equivalently a smaller mismatch), the peak shift effect will be more apparent. We note that the angular positions of the higher-order SL peaks (only the zeroth- and the first-order peaks are shown here) are not changed with the changing thickness. The IBC kinematical calculation, however, is unable to exhibit the peak shift effect as Fig. 5(d) shows, in agreement with Tapfer's observation.[26] Because the kinematical approximation is valid only for a total thickness that is below the x-ray primary extinction length and because the peak shift effect can occur in this thickness range, the IBC kinematical model will not properly simulate the experimental diffraction profile of the zeroth-order SL peak and should not be used for such analyses. In Fig. 5(a), the experimental rocking curves were obtained after a successive chemical etching. The four rocking curves agree with a SL period of 50, 28, 12, and 7, respectively.

Finally, we briefly discuss the significance of the zeroth-order SL peak profile in the superlattice analysis. The angular shift of the zeroth-order SL peak is important because its angular separation $\Delta\theta_0$ from the substrate peak determines the average lattice mismatch and therefore the average chemical composition of the SL as can be seen from

$$\Delta\theta_0 = -k_\perp \langle \epsilon_\perp \rangle - k_\parallel \langle \epsilon_\parallel \rangle, \tag{10}$$

where the angular bracket means an average over the SL period and the quantities in the angular brackets are the perpendicular and parallel mismatches of the SL layers relative to the substrate lattice. Considering the peak shift effect, a detailed fitting analysis of the experimental data is necessary to obtain more accurate information on the layer composition and mismatch using either the dynamical theory or the ABC kinematical model. As for the SL period thickness, the

angular separation between higher-order SL peaks (i.e., not including the zeroth-order peak) will yield more accurate information because their positions are not affected by the peak shift effect which occurs in the zeroth-order peak.

## IV. CONCLUSIONS

We have introduced a kinematical x-ray-diffraction model with a new boundary condition. The new boundary condition employs the dynamical complex amplitude instead of the dynamical intensity of the substrate. Using this boundary condition, we have shown that the kinematical diffraction model can properly simulate the peak shift effect in the Bragg-peak profile of a single epitaxial layer sample and in the zeroth-order SL peak. The kinematical models (both ABC and IBC) can be used to analyze the interference profile in the $C$-layer Bragg peak of the $C/A/C/sub$-type samples, but not in the $B$-layer Bragg peak of the $B/A/B$-type samples where the $A$ layer is a strained pseudomorphic layer. This is because the two layers (one of which can be the substrate) that produce the Bragg peak in which the interference profile is formed must both have either the dynamical expression or the kinematical expression. In the kinematical model (whether ABC or IBC), however, the substrate is from the dynamical theory whereas the layers are from the kinematical model. With the use of the new boundary condition, the kinematical model can be safely used for the simulation study of rocking curves of most of the thin layer samples. We have also presented a matrix method of superlattice rocking curve calculation using the dynamical theory. The matrix method was found to be more efficient than the recursive formula approach for a large period SL and for investigating the interfacial layer effect in the rocking curves.


## ACKNOWLEDGMENTS

This work was supported in part by the National Science Foundation under Grants No. DMR-8857403 and No. ECS-8913229. One of us (C.R.W.) is a National Science Foundation Presidential Young Investigator.


## APPENDIX

A useful solution to the Takagi–Taupin equation is given by a ratio of the diffracted displacement field ($D_H$) to the incident displacement field ($D_0$) as a function of depth into the crystal ($z$),[12]

$$X(z) \equiv D_H(z)\sqrt{|\gamma_H|}/D_0(z)\sqrt{|\gamma_0|}, \tag{A1}$$

where $\gamma_0$ and $\gamma_H$ are the direction cosines of the incident and diffracted wave vectors with respect to the inward surface normal. In the Bragg case, an analytic solution is given by

$$X(z_j) = \frac{S_j X(z_{j-1}) + i[B_j + C_j X(z_{j-1})]\tan[S_j A_j (z_j - z_{j-1})]}{S_j - i[C_j + B_j X(z_{j-1})]\tan[S_j A_j (z_j - z_{j-1})]}, \tag{A2}$$

where $j$ is the layer number, numbered upward from the substrate (the substrate is $j=0$), and $z_j$ is the depth at the top surface of the $j$th layer, measured from the sample surface (see Fig. 6). This formula applies to the $\sigma$-state polarization only. For the $\pi$-state polarization, corresponding results can be obtained by everywhere replacing $F_H$ by $F_H \cos 2\theta_B$.[31] Other parameters in Eq. (A2) are defined as follows:

$$A = \lambda r_e F'_H / V\sqrt{|\gamma_0 \gamma_H|}, \quad B = -F_H/F'_H,$$

$$C = Y + ig, \quad S = \sqrt{C^2 - B^2},$$

$$Y = -[(1+b)F'_0 + (\pi V/\lambda^2 r_e) b\alpha_H]/2|F'_H|\sqrt{b},$$

and

$$g = -(1+b)F''_0/2F'_H\sqrt{b}.$$

Here, $\alpha_H$ is a measure of the angular deviation from the Bragg angle,

$$\alpha_H = -2(\theta - \theta_B)\sin 2\theta_B - 2(k_\perp \epsilon_\perp + k_\parallel \epsilon_\parallel)\sin 2\theta_B,$$

where $\theta_B$ is the substrate Bragg angle, $b$ is the ratio of direction cosines given by

$$b = |\gamma_0/\gamma_H|,$$

$k_\perp$ and $k_\parallel$ are geometrical factors, respectively given by

$$k_\perp = \cos\varphi \tan\theta_B - \sin\varphi\cos\varphi,$$

$$k_\parallel = \sin\varphi \tan\theta_B + \sin\varphi\cos\varphi,$$

$\epsilon_\perp$ and $\epsilon_\parallel$ are the plane-normal and in-plane lattice mismatches, respectively, given by

$$\epsilon_\perp = (a_\perp - a_s)/a_s, \quad \epsilon_\parallel = (a_\parallel - a_s)/a_s,$$

$\varphi$ is the angle between the reflecting lattice plane and the sample surface, $F_{0,H} = F'_{0,H} + iF''_{0,H}$ is the structure factor for the incident (0) and diffracted ($H$) waves, $\theta + \varphi$ is the grazing angle of incidence, $r_e$ is the classical electron radius, $V$ is the unit-cell volume, $\lambda$ is the x-ray wavelength, $a_\perp$ and $a_\parallel$ are the layer lattice constants normal and parallel to the interface, respectively, and $a_s$ is the substrate lattice constant.

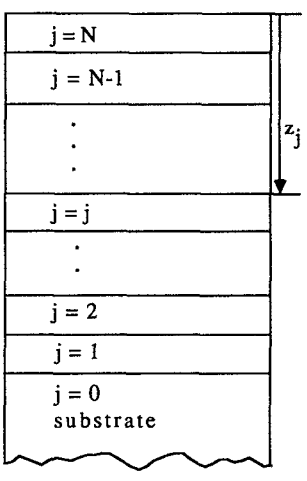


FIG. 6. Sample schematics showing the convention for layer number and depth.

[1] W. J. Bartels and W. Nijman, J. Cryst. Growth **44**, 518 (1978).
[2] L. Tapfer and K. Ploog, Phys. Rev. B **33**, 5565 (1986).
[3] P. F. Fewster and C. J. Curling, J. Appl. Phys. **62**, 4154 (1987).
[4] S. Bensoussan, C. Malgrange, and M. Sauvage-Simkin, J. Appl. Cryst. **20**, 222 (1987).
[5] T. Baumbach, H.-G. Bruhl, H. Rhan, and U. Pietsch, J. Appl. Cryst. **21**, 386 (1988).
[6] V. S. Speriosu and T. Vreeland, Jr., J. Appl. Phys. **56**, 1591 (1984).
[7] W. J. Bartels, J. Hornstra, and D. J. W. Lobeek, Acta Cryst. A **42**, 539 (1986).
[8] J. Kervarec, M. Baudet, J. Caulet, P. Auvray, J. Y. Emery, and A. Regreny, J. Appl. Cryst. **17**, 196 (1984).
[9] D. M. Vardanyan, H. M. Manoukyan, and H. M. Petrosyan, Acta Cryst. A **41**, 212 (1985).
[10] A. Fukuhara and Y. Takano, Acta Cryst. A **33**, 137 (1977).
[11] J. Burgeat and D. Taupin, Acta Cryst. A **24**, 99 (1968).
[12] B. C. Larson and J. F. Barhorst, J. Appl. Phys. **51**, 3181 (1980).
[13] V. S. Speriosu, B. M. Paine, M.-A. Nicolet, and H. L. Glass, Appl. Phys. Lett. **40**, 604 (1982).
[14] C. R. Wie, T. A. Tombrello, and T. Vreeland, Jr., J. Appl. Phys. **59**, 3743 (1986).
[15] T. Takeuchi, N. Ohta, Y. Sugita, and A. Fukuhara, J. Appl. Phys. **54**, 715 (1983).
[16] J. Miltat, IEEE Trans. Magn. **MAG-20**, 1114 (1984).
[17] C. R. Wie, J. C. Chen, H. M. Kim, P. L. Liu, Y.-W. Choi, and D. M. Hwang, Appl. Phys. Lett. **55**, 1774 (1989).
[18] L. Tapfer, M. Ospelt, and H. von Kanel, J. Appl. Phys. **67**, 1298 (1990).
[19] K. M. Yu and K. T. Chan, Appl. Phys. Lett. **56**, 45 (1990).
[20] C. R. Wie, Nucl. Instrum. Methods B **37/38**, 965 (1989).
[21] A. Segmuller, Thin Solid Films **154**, 33 (1987).
[22] H. Rhan and U. Pietsch, Phys. Status Solidi A **107**, K93 (1988).
[23] S. Takagi, Acta Cryst. **15**, 1311 (1962); D. Taupin, Bull. Soc. Franc. Miner. Cryst. **87**, 469 (1964).
[24] M. A. G. Halliwell, M. H. Lyons, and M. J. Hill, J. Cryst. Growth **68**, 523 (1984).
[25] V. S. Speriosu, J. Appl. Phys. **52**, 6094 (1981).
[26] L. Tapfer, Phys. Scr. T**25**, 45 (1989).
[27] C. R. Wie, J. Appl. Phys. **66**, 985 (1989).
[28] R. M. Fleming, D. B. McWhan, A. C. Gossard, W. Wiegmann, and R. A. Logan, J. Appl. Phys. **51**, 357 (1980).
[29] C. R. Wie, J. Appl. Phys. **65**, 1036 (1989).
[30] H. Holloway, J. Appl. Phys. **67**, 6229 (1990).
[31] W. H. Zachariasen, *Theory of X-Ray Diffraction in Crystals* (Wiley, New York, 1945), p. 117.
[32] Reference 25 used the dynamical intensity of the substrate as the boundary condition and therefore we name his formula the intensity boundary condition (IBC) formula.
[33] A. T. Macrander, E. R. Minami, and D. W. Berreman, J. Appl. Phys. **60**, 1364 (1986).
[34] D. W. Berreman, Phys. Rev. B **14**, 4313 (1976).
[35] L. Tapfer and K. Ploog, Phys. Rev. B **40**, 9802 (1989).